JOURNAL OF MATERIALS SCIENCE: MATERIALS IN MEDICINE, 7 (1996) 323–329

Characterization of titanium alloy implant surfaces with improved dissolution resistance

M. BROWNE*, P. J. GREGSON*, R. H. WEST‡
*Engineering Materials, University of Southampton, Southampton, SO17 1BJ, UK
‡CSMA Ltd., Armstrong House, Oxford Road, Manchester, M1 7ED, UK

The present work sets out to investigate the structure and chemistry of surface treated oxides (either aged in boiling water or air-heated) with improved dissolution resistance compared to conventionally passivated surfaces. X-ray photoelectron spectroscopy (XPS) has demonstrated a significant reduction in oxidized aluminium associated with an ageing-based surface treatment. Angle-dependent XPS has revealed an increase in amphoteric-OH surface sites for the thermal treatments. Atomic force microscopy (AFM) investigation suggests that these sites play a role in the improved protein adsorption properties of these surfaces. These observations form the basis of a model which describes the influence of surface oxide on the kinetics of metal ion dissolution.

1. Introduction

Implant materials used in total hip arthroplasty usually undergo some form of cleaning/surface treatment such as nitric acid passivation during commercial fabrication. It has been shown that *in vitro* metal ion release from nitric acid passivated titanium alloy implants is reduced considerably when simple thermal treatments such as ageing in de-ionized water or heating in air are applied before immersion into both an EDTA/saline and bovine serum environment [1–3]. This reduction in metal ion release is attributed to a conversion in the surface oxide to a stable homogeneous rutile structure.

Previous work has concentrated on studies of the bulk oxide coating, but dissolution of metal ions occurs via complex reactions at the implant/bioenvironment interface, the kinetics of the process being controlled by the physical and chemical properties at the prosthesis surface. X-ray photoelectron spectroscopy (XPS) has been used widely as a technique for identifying the surface chemistry of surface oxides [4–9]. A knowledge of the surface chemistry will contribute greatly to the understanding of (i) the dissolution process and (ii) the mechanism by which the biomaterial will interact with the bioenvironment in order to create a suitable transition zone for bone growth.

It has been postulated that reorganization of the tissue adjacent to titanium implants depends on adsorption of proteins from the liquid initially separating the implant and tissue [10]. Thus the probability of adsorption will depend upon favourable conditions being prevalent at the surface; further growth of surrounding tissue will depend on whether the protein altered surface is attractive to the encroaching tissue. It is probable that a dynamic situation exists where a continual exchange of proteins occurs, with some becoming adsorbed preferentially [11]. The present work sets out to investigate more closely the surface chemistry in order to understand more fully the low dissolution rates associated with the thermally treated surfaces.

2. Experimental procedures

Distal sections of forged Ti-6Al-4V titanium alloy femoral stems from the Ti-Mod Freeman hip replacement made to BS7252 Part 3 were sectioned and polished to a 1 μm finish. They were then treated to provide different oxide surface conditions:

(i) immersed in 30% nitric acid for 10 min (treatment C);
(ii) immersed in 30% nitric acid for 16 h (N);
(iii) heated in air at 400 °C for 45 min (T);
(iv) aged in boiling de-ionized water for 10 h (A).

Metal ion dissolution was monitored with time in bovine serum at 37 °C, according to the procedure documented elsewhere [2].

X-ray photoelectron spectroscopy (XPS) was carried out for each of the four surface treatments. All analyses were carried out using a Surface Science Instruments M-Probe operating at a base pressure of 4×10^{-7} Pa and using a spot size of 400 μm × 1000 μm. More detailed scans were made at the binding energies corresponding to the titanium peaks. High resolution scans of the thermally treated samples were curve fitted and the species present on the oxide surface identified. High resolution angle dependent XPS scans were made for the oxygen peaks found on the aged sample.

Atomic force microscopy (AFM), has been used for *in situ* examination of non-conducting surfaces in an ambient environment [12, 13]. The use of such a technique should allow surface processes such as

0957–4530

adsorption to be followed. A topographic image of both the passivated and aged sample was produced using atomic force microscopy (AFM). Samples were immersed in bovine serum at 37 °C for 0, 20 and 200 h and ultrasonically cleaned in double distilled water to remove any weakly adsorbed proteins from the serum, dried and scanned at a constant force (1.5×10^{-9} N).

3. Results

3.1. Surface chemistry

XPS traces for each of the four surface treatments are shown in Fig. 1. The scans for both the short and extended nitric acid passivated treatments (C and N) were very similar, with no indication of the presence of vanadium. Aluminium was in evidence with a trace of nitrogen and a significant carbon signal is present at a specific binding energy, indicating the presence of C–O, C=O and O–C=O organic species on the surfaces. The same elemental species are present on the air-heated oxide with the addition of trace quantities of calcium and zinc. The aged oxide surface scan, however, shows the elimination of an aluminium peak. A summary of the elemental compositions are given in Table I.

A comparison of the Ti 2p peaks resulting from each treatment is given in Table II. Both the short and extended passivation treatments result in a similar titanium peak at 458.6 eV corresponding to TiO_2. However, the thermally treated samples (A and T) show a noticeable difference: the titanium peak is shifted to a lower binding energy of 458.1 eV. A typical XPS scan of the Ti 2p peak for the ageing treatment is shown in Fig. 2.

High resolution titanium scans for the thermal treatments (Fig. 3) indicate further species at the higher binding energy edge. These species can clearly be identified as two separate entities on the oxygen trace, and their contribution increases at shallower angles of incidence (Fig. 4), that is, at the outermost surface.

3.2. Surface morphology

The surface morphology of samples immersed in serum for 0, 20 and 200 h studied in the AFM reveal a distinct difference (Figs 5 and 6). After 20 h immersion, colonies of adsorbed species begin to appear on the aged samples. There appears to be no adsorption processes occurring on the passivated samples even after 200 h immersion. After 200 h immersion, the colonies on the aged surfaces appear to have spread over the whole surface in coverage (Fig. 6c). Ridges which are not seen on the non-immersed samples are evidence of the growth of the biolayer.

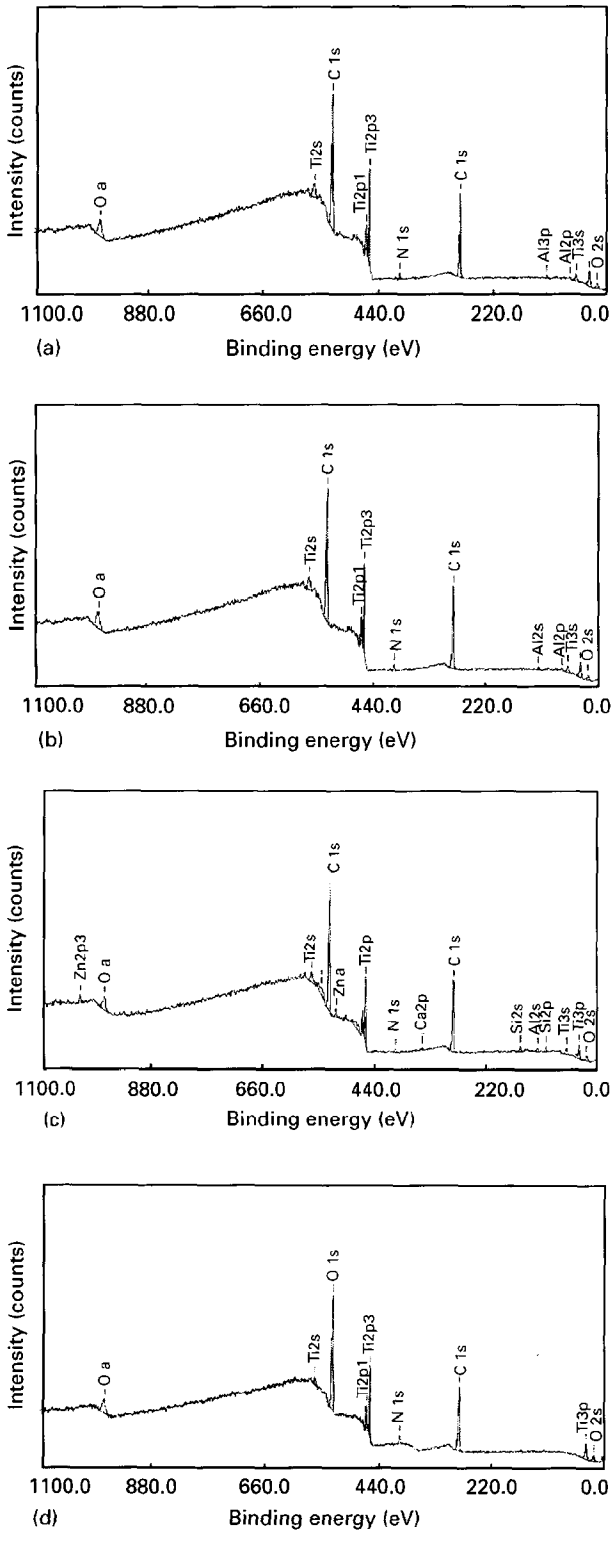

Figure 1 (a) Standard angle (35°) scan for short passivation treatment (C). (b) Standard scan for extended passivation treatment (N). (c) Standard scan for air heated treatment (T). (d) Standard scan for ageing teatment (A).

4. Discussion

4.1. Kinetics of dissolution

Using the results presented previously [2], a model describing the kinetics of the dissolution process can be established using a few simple assumptions: (i) the concentration of the metal ions at the metal oxide/solution interface is constant; (ii) the concentration of metal ions in the liquid is negligible compared to that at the metal oxide/solution interface; and (iii) metal diffusion through a boundary layer at the oxide/liquid interface is the rate-controlling step. Thus, the rate of growth of this boundary layer dS/dt is proportional to the flux of dissolution product through it, which is proportional to $D \cdot \Delta C/\Delta X$ where $\Delta C/\Delta X$ is the concentration gradient ($\approx C(x = 0)/S(t)$).

TABLE I Elemental composition of oxide

Element	Binding energy (eV)	Composition (at %)
After commercial passivation treatment (C)		
Titanium	458.2	9.4
Aluminium	118.2	2.4
Oxygen	530.2	39.6
Carbon	284.9	45.9
Nitrogen	400.0	2.7
After extended passivation treatment (N)		
Titanium	458.2	11.4
Aluminium	118.2	3.7
Oxygen	530.2	39.7
Carbon	284.9	42.5
Nitrogen	400.0	2.6
After air heating treatment (T)		
Titanium	458.2	9.4
Aluminium	118.2	2.4
Oxygen	530.2	39.6
Carbon	284.9	45.9
Nitrogen	400.0	2.7
Calcium	347.2	1.01
Zinc	1021.5	0.52
After ageing treatment (A)		
Titanium	458.2	7.62
Aluminium	118.2	0.67
Oxygen	530.2	34.59
Carbon	284.9	52.69
Nitrogen	400.0	3.49

TABLE II Ti 2p3 peak binding energy and relative areas for various surface treatments

Surface treatment	Ti 2p3 Peak energy (eV)	Peak area
Short passivation (C)	458.60	7424
Extended passivation (N)	458.69	7917
Air heated (T)	458.23	5938
Aged 100 °C in water (A)	458.15	4152

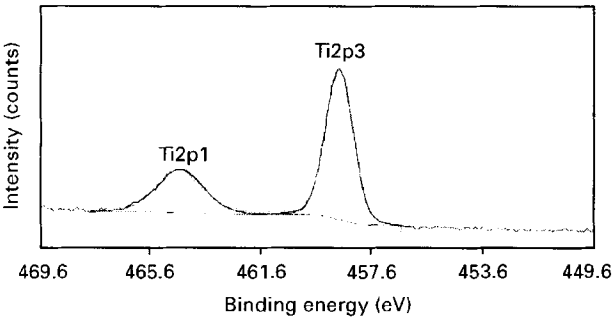

Figure 2 Typical XPS trace for Ti 2p peak after surface treatment: aged sample (A).

Thus

$$dS/dt = A D C(x = 0)/S(t)$$

and it follows that

$$S = K t^{1/2}$$

Therefore the total concentration of metal atoms in the liquid should be proportional to S, (i.e., to $t^{1/2}$) and

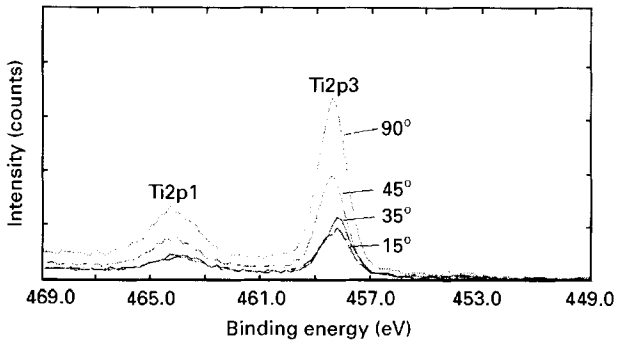

Figure 3 Titanium spectra collected at four incident angles.

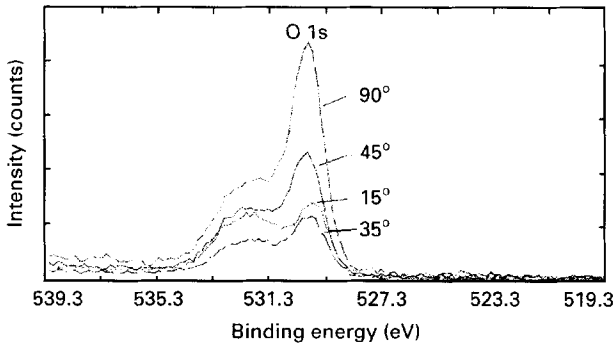

Figure 4 Oxygen spectra collected at four incident angles.

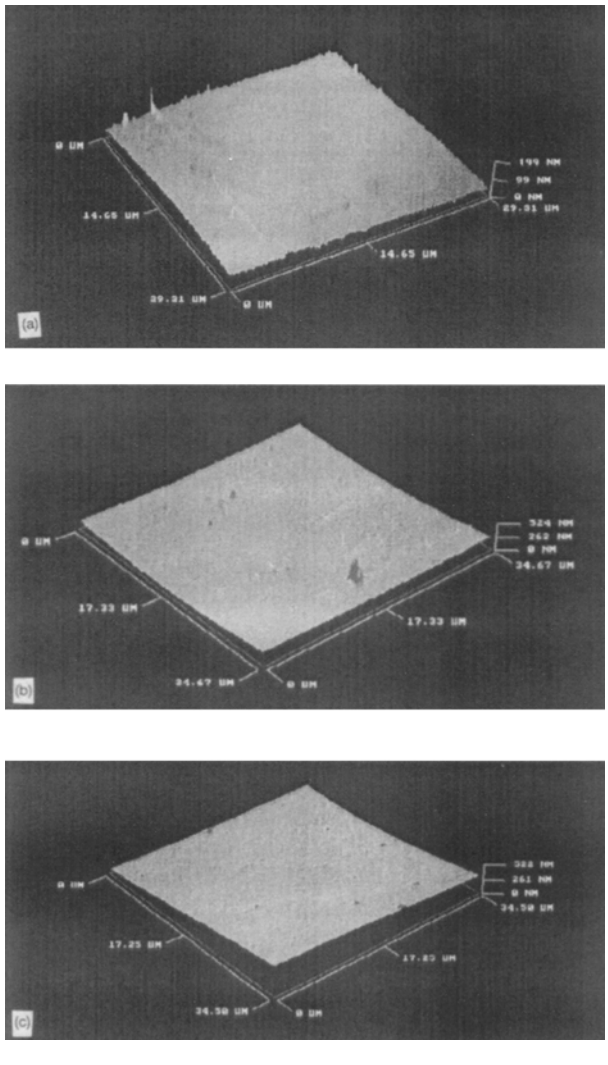

Figure 5 Passivated sample (a) before immersion; (b) after 20 h immersion; (c) after 200 h immersion.

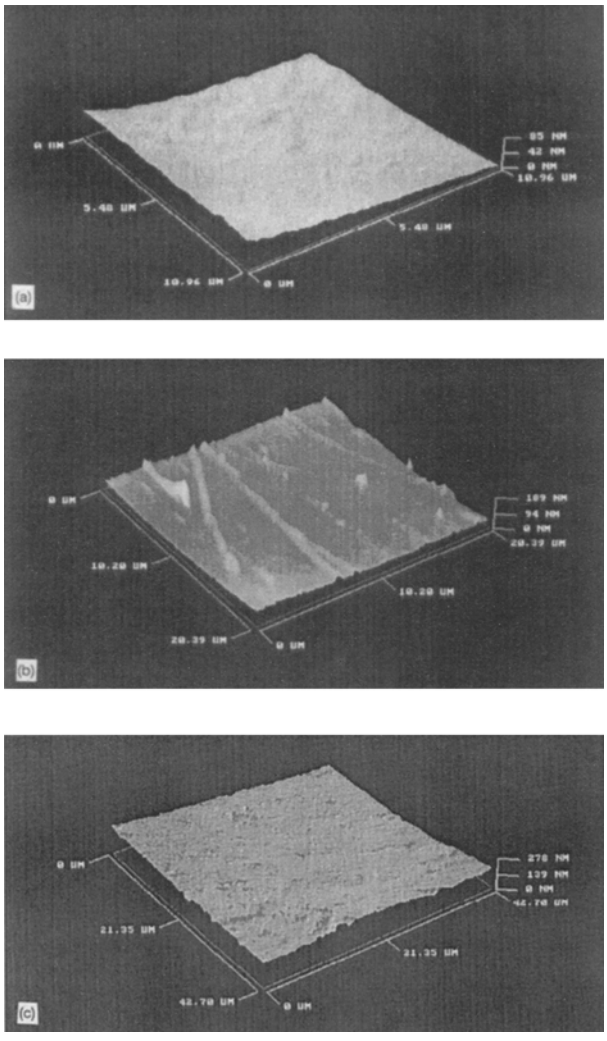

Figure 6 Aged sample (a) before immersion; (b) after 20 h immersion; (c) after 200 h immersion.

the rate of metal ion release should be proportional to dS/dt (i.e., to $t^{-1/2}$).

Figs 7 and 8 show the concentration of aluminium and titanium metal ions released into serum as a function of $t^{1/2}$ for the various surface treatments. A straight line relationship is followed for both the nitric acid passivation treatments indicating dissolution is a diffusion controlled process. For the thermal treatments, two kinetic stages are observed: an initial low rate for short exposure times and a subsequent very low rate under long term exposure (Table III). Interpretation of such complex dissolution mechanisms requires a detailed understanding of the structure, chemistry and surface reactions of the oxide film, determined by TEM, XPS and AFM.

Transmission electron microscopy (TEM) has characterized the bulk surface oxide [1, 2] and shown that thermal treatments result in the formation of a stable rutile oxide structure. This would account for the initial low dissolution rates observed for these treatments (Table III). X-ray photoelectron spectroscopy (XPS), is a surface-sensitive technique which provides information on the chemical environment of the surface groups which will be in contact with the bioenvironment. The XPS traces for the passivated and thermally treated oxides revealed notable differences: The nitric acid passivated treatments show a shift in the Ti 2p peak position compared with the thermally treated samples. The standard treatments show the titanium peak at a binding energy of 458.6 and 458.7 eV, respectively, corresponding to the anatase form of TiO_2 as observed by TEM [2]. However, the thermal treatments result in a Ti 2p peak at 458.1 and 458.2 eV respectively. TEM has shown that this oxide is the rutile form of TiO_2 [1, 2]. Nitric acid passivated samples possess a thin defective oxide layer analogous to that observed previously for Al_2O_3 by Ocal *et al.* who studied the effect of oxygen exposure on thin, defective aluminium oxide layers [14]. They noted a similar shift in binding energy upon oxygen exposure and attributed this to a stabilization of an anionic oxygen layer on the surface which produced an electrostatic potential between itself and its cationic counterpart at the metal–oxide interface (Fig. 9). This anionic oxygen layer may serve to attract species from the bioenvironment such as calcium containing macromolecules [21]. Ocal *et al.* have also noted a decrease in the Al 2p peak on exposure to oxygen. A similar decrease is seen for the thermal Ti 2p peaks (Fig. 2).

A major finding for those samples aged in boiling water is the reduction in aluminium signal to a trace level. The presence of aluminium in the outer layers of air heated oxides has been confirmed by other workers [4, 5]. The polarization caused by the aluminium will differ from that of the native titanium ions, with the electropositive aluminium ion more likely to react, for example, with adsorbed water. However, in the absence of aluminium oxide, the potential for aluminium dissolution is reduced considerably and this is reflected in the dissolution behaviour of the aged samples [1–3].

High resolution scans of the titanium peak for both types of thermally treated sample show a slight deviation from the Gaussian fit at the lower binding energy edge of the peak. This observation suggests that additional titanium containing species are present at the oxide surface. Metal oxide surfaces such as titanium oxide become hydrated when exposed to ambient moisture. Hydration minimizes the surface potential and amphoteric OH sites are formed. In the case of TiO_2, basic and acidic OH groups are formed by chemisorption, their chemical nature arising from the way in which they are bound, either to one or two titanium ions (Fig. 10). Shams and Lazarus have examined the XPS spectra of hydrated TiO_2 [7], and have attributed structure on the leading edge of the Ti $2p_{3/2}$ peak to Ti-OH. The work took place on bulk TiO_2, however, thin oxidized films have been investigated on pure titanium and alloy films by Lee *et al.* [23] where suboxide states were identified at the interface between very thin oxide films and the parent metal. Their observations concluded that after exposure to atmosphere for a few minutes the oxide layer thickness was several times the escape depth of XPS and that the reactions taking place with oxygen and water were controlled by the properties of the oxide and not the metal substrate. The peak observed by Shams and Lazarus occurs at a binding energy of

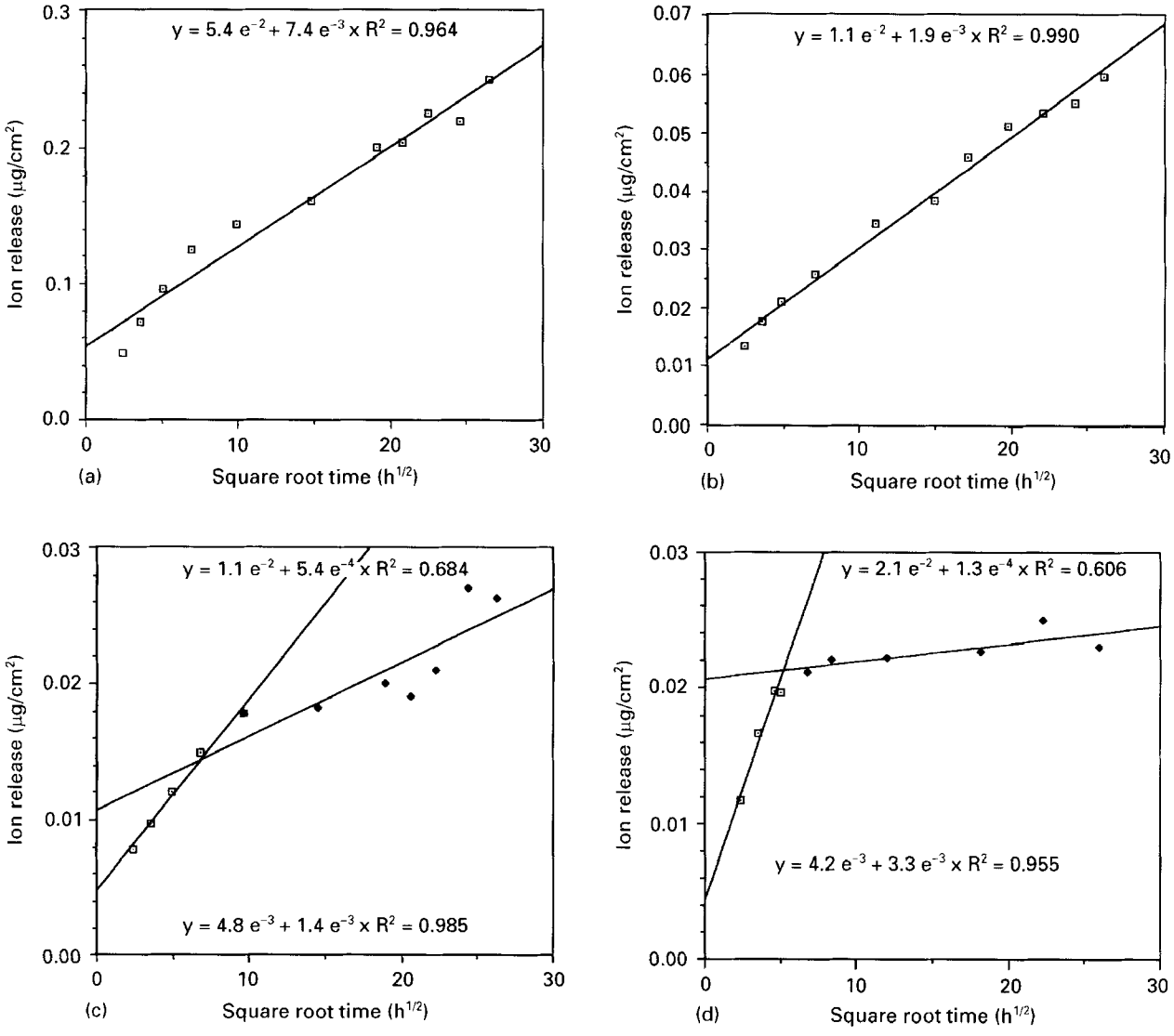

Figure 7 Single-stage aluminium ion release kinetics for (a) short (commercial) passivation specimen; (b) extended passivation specimen. Two-stage aluminium ion release kinetics for (c) air heated sample; (d) aged sample. A least squares fit is shown for each kinetic regime.

457.9 eV, similar to the titanium peak found for thermally treated samples, and is attributed to hydration of the metal oxide surface. They found that this deviation occurred at a high angle of incidence to the oxide surface, and the hydration peak increased at a near grazing incidence, that is, at the outermost surface layers. This is clearly seen on the low angle oxygen trace for the aged sample (Fig. 11). Acidic and basic OH peaks can clearly be identified. The magnitude of these peaks increases at shallower angles of incidence, and is greater than those observed by other workers [7, 15, 16], suggesting a high concentration of these groups at the outermost oxide surface. These groups may play an important role in oxide/biomolecule integration. It has been shown that acidic hydroxyl groups tend to act as cation exchange sites, while basic hydroxyl groups may act as anion exchange sites [18, 19]. It has been suggested that calcium ions may bind with these acidic groups, and phosphate molecules with the basic groups [16]. These may in turn react with calcium and phosphate binding biomolecules to begin the development of a suitable transition zone for bone growth. The encouragement of protein/biomolecule adsorption reactions, will aid in the formation of a surface biolayer which will reduce the transport of dissolution products away from the implant surface. This would explain the ion release behaviour exhibited by the thermally treated oxides, which show a negligible ion release rate after approximately 200 h [2]. This is in contrast to similar experiments in EDTA/saline solution which show an increase in ion release with time, for which no adsorption processes appear to occur [1, 3].

Atomic force microscopy (AFM) has clearly revealed an increase in "biolayer" coverage with time for the aged sample, similar to an increase in protein adsorption with time observed previously for rutile crystals [20]. The thicker, air-heated samples would be expected to behave in a similar manner. The graphs of concentration versus $t^{1/2}$ show two kinetic phases. Up to 100 h there is a low ion release rate associated with these samples. This will simply be due to the dissolution resistant rutile surface oxide. It would appear that complete coverage of the surface occurs after approximately 150 h, at the beginning of the second kinetic phase, at which time ion release from these

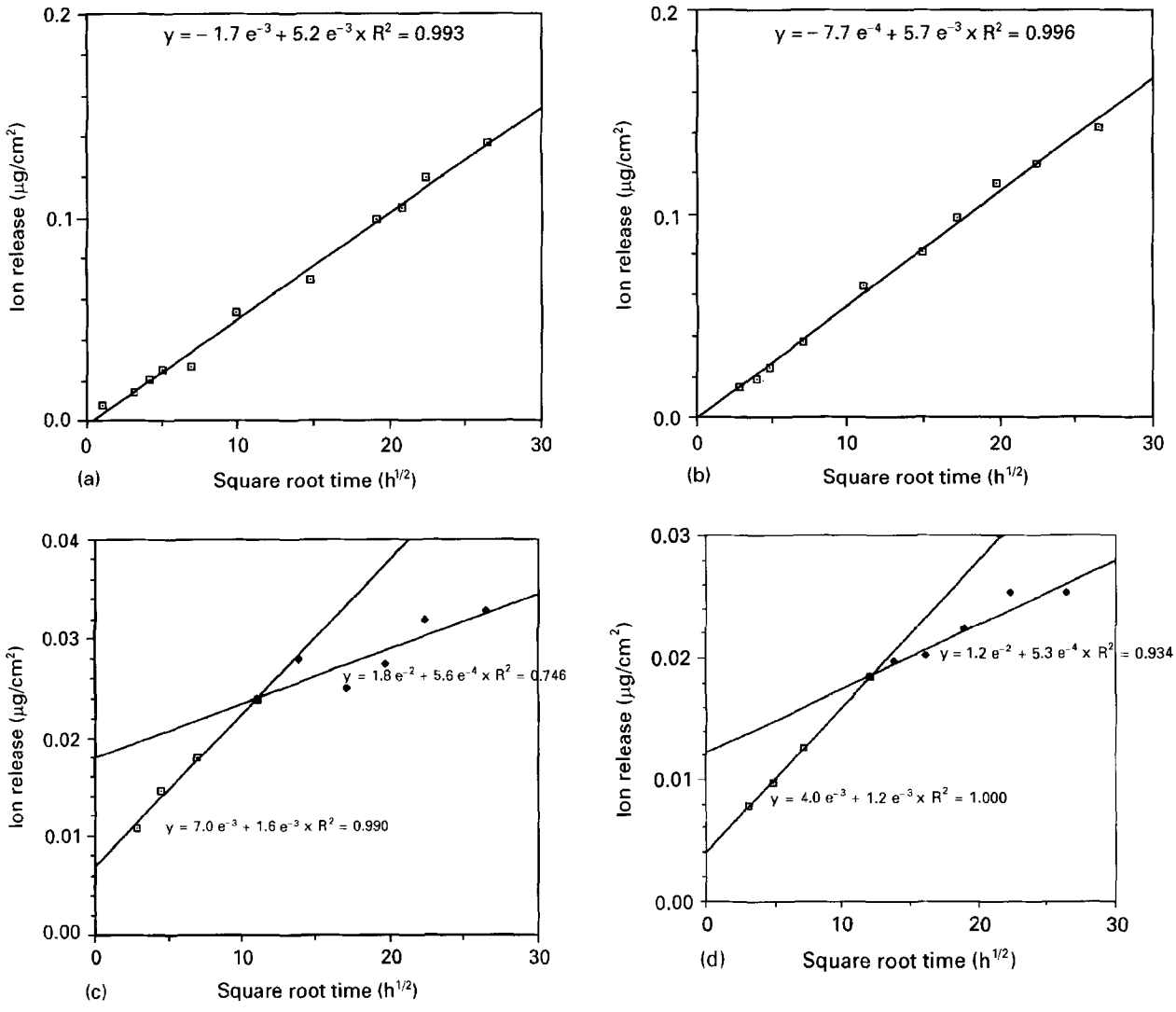

Figure 8 Single-stage titanium ion release kinetics for (a) short (commercial) passivation specimen. (b) extended passivation specimen. Two-stage titanium ion release kinetics for (c) air heated sample; (d) aged sample.

TABLE III Kinetic rate constants for metal ion release into bovine serum

Surface treatment	Rate constant (stage I) ($\mu g/cm^2/h^{1/2}$)	Rate constant (stage II) ($\mu g/cm^2/h^{1/2}$)
Aluminium		
Nitric acid passivated (C)		5.2×10^{-3}
Nitric acid passivated (N)		5.7×10^{-3}
Air heated 400 °C (T)	1.4×10^{-3}	5.4×10^{-4}
Aged boiling water (A)	3.3×10^{-3}	1.3×10^{-4}
Titanium		
Nitric acid passivated (C)		7.4×10^{-3}
Nitric acid passivated (N)		1.9×10^{-3}
Air heated 400 °C (T)	1.6×10^{-3}	5.6×10^{-4}
Aged boiling water (A)	1.2×10^{-3}	5.3×10^{-4}

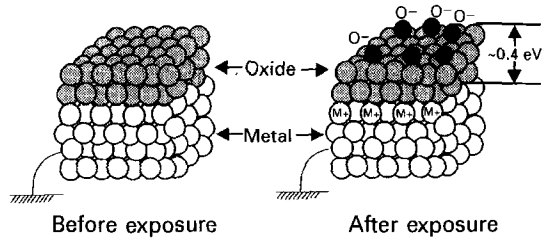

Figure 9 Stabilization of an anionic layer on the surface of a thin oxide exposed to oxygen (after Ocal *et al.* [14]).

surfaces is negligible [2]. Thus, the formation of a diffusion limiting "biolayer" alters the formation and transport of dissolution products away from the implant surface resulting in an extremely low ion release rate. The passivated samples show a linear relationship throughout the experiment time, indicating a diffusion controlled process is occurring. AFM reveals an absence of significant adsorption processes occurring, and the diffusion controlled process will be taking place through the surface boundary layer. The absence of a diffusion limiting biolayer results in a higher release rate and this treatment is seen as relatively non-protective compared to the thermal treatments.

It would appear therefore, that the existence of the amphoteric –OH groups on the thicker thermally treated samples is beneficial in attracting proteinous species from the bioenvironment to form a biolayer. These observations appear to confirm the findings of Li *et al.* who suggested that the creation of abundant

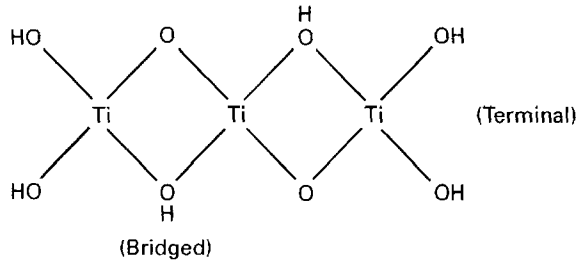

Figure 10 Bridged and terminal hydroxyl sites on the titania surface.

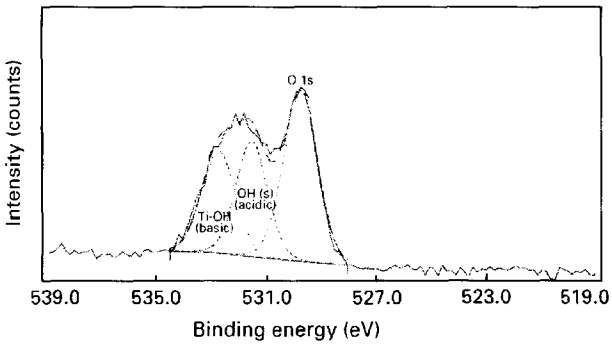

Figure 11 Oxygen spectra collected at shallow angle. Model: Gaussian; asymmetry: 0.00; χ^2:1.93.

Energy	Width	Area	%
529.75	1.46	12730	45.4
531.4	1.33	7905	28.2
532.74	1.41	7407	26.4

TiOH groups is a factor in promoting bone bonding on titanium and its alloys [22].

A combination of TEM and XPS has revealed two factors which describe the improved dissolution resistance with the thermal treatments. TEM has shown a rutile structure forms on the implant surface, which itself is the most stable form of TiO_2, and XPS has revealed a hydrated surface with amphoteric –OH sites, which assists the formation of a diffusion limiting biolayer.

5. Conclusions

Thermal treatments of titanium alloy implants results in a slight shift in XPS binding energy for the titanium 2p peak, suggesting the formation of a stable anionic surface layer. A reduction in peak height also occurs, indicating the formation of a more stoichiometric oxide. The aged sample has revealed a drastic reduction in signal for oxidized aluminium from the outermost oxide surface, reducing its potential for dissolution.

Angle-dependent XPS has revealed an extremely hydrated aged oxide surface with amphoteric –OH sites. AFM has confirmed that these sites act as preferred sites for implant/bioenvironment integration. It is postulated that a biolayer is established which lowers the rate of formation and transport of dissolution product away from the implant site, resulting in a lower metal ion concentration in the serum environment.

Acknowledgements

The authors would like to thank the Arthritis and Rheumatism Council for Research for their financial assistance and Mr M. Tuke of Finsbury Instruments, Leatherhead, Surrey, for the supply of hip replacement stems used in this work.

References

1. A. WISBEY, PhD thesis, University of Southampton, 1990.
2. M. BROWNE and P. J. GREGSON, *Biomaterials* **15** (1994) 894.
3. A. WISBEY, P. J. GREGSON, L. M. PETER and M. TUKE, *Biomaterials* **12** (1991) 470.
4. M. ASK, J. LAUSMAA and B. KASEMO, *Appl. Surf. Sci.* **35** (1988–1989) 283.
5. K. W. VOGT, P. A. KOHL, W. B. CARTER, R. A. BELL and L. A. BOTTOMLEY, *Surf. Sci.* **301** (1994) 203.
6. G. BLONDEAU, M. FROELICHER, M. FROMENT and A. HUGOT-LE GOFF, *J. Less Common Metals* **56** (1977) 215.
7. T. K. SHAM and M. S. LAZARUS, *Chem. Phys. Lett.* **68** (1979) 426.
8. P. A. MAEUSLI, P. R. BLOCH, V. GERET and S. G. STEINEMANN, in "Biological and biomechanical performance of biomaterials", edited by P. Christel, A. Meunier, and A. J. C. Lee, (Elsevier Science Publishers Amsterdam, 1986) p. 57.
9. J. LAUSMAA, M. ASK, U. ROLANDER and B. KASEMO, *Mater. Res. Symp. Proc.* **110** (1989) 647.
10. B. KASEMO and J. LAUSMAA, in *CRC Crit. Rev. Biocomp.*, edited by D. F. Williams, (CRC Press, Boca Raton, FL 1986) p. 335.
11. B. IVARSSON and I. LUNDSTROM, in *CRC Crit. Rev. Biocomp.*, edited by D. F. Williams, (CRC Press, Boca Raton, FL 1986) p. 1.
12. G. BINNIG, C. F. QUATE and C. H. GERBER, *Phys. Rev. Lett* **56** (1986) 930.
13. P. K. HANSMA, V. B. ELINGS, O. MARTI and C. E. BRAKER, *Science* **242** (1988) 209.
14. C. OCAL, S. FERRER and N. GARCIA, *Surf. Sci.* **163** (1985) 335.
15. L.-J. MENG, C. P. MOREIRA DE DA and M. P. DOS SANTOS, *Thin Solid Films* **239** (1994) 117.
16. K. E. HEALY and P. DUCHEYNE, *Biomaterials* **13** (1992) 553.
17. H. P. BOEHM, *Adv. Catal.* **16** (1966) 249.
18. J. RAGAI and S. I. SELIM, *J. Colloid Interf. Sci.* **115** (1987) 139.
19. J. P. BONSACK, *ibid.* **44** (1973) 430.
20. R. L. WILLIAMS and D. F. WILLIAMS, *ibid.* **126** (1988) 596.
21. J. E. ELLINGSEN, *Biomaterials* **12** (1991) 593.
22. P. LI, C. OHTSUKI, T. KOKUBO, K. NAKANISHI, N. SOGA and K. DE GROOT, *J. Biomed. Mater. Res.* **28** (1994) 7.
23. P. A. LEE, K. F. STORK, B. L. MASCHOFF, K. W. NEBENSY and N. R. ARMSTRONG, *Surf. and Interf. Anal.* **17** (1991) 48.

Received 28 June
and accepted 7 September 1995